Analysis of the Ligand Binding Site in Fas (CD95) by Site-Directed Mutagenesis and Comparison with TNFR and CD40

Gary C. Starling,* Peter A. Kiener, Alejandro Aruffo, and Jürgen Bajorath‡

Bristol-Myers Squibb Pharmaceutical Research Institute, 3005 First Avenue, Seattle, Washington 98121, and BMS-PRI and Department of Biological Structure, University of Washington, Seattle, Washington 98195

Received December 2, 1997

ABSTRACT: Fas and its ligand (FasL) are members of the tumor necrosis factor receptor (TNFR) and tumor necrosis factor (TNF) superfamilies, respectively. Fas−FasL interactions trigger controlled cell death (apoptosis) in the immune system and thus play a key role in the regulation of immune responses. Structural details of the Fas−Fas ligand interaction are currently unknown. Previously, six Fas residues were identified by mutagenesis as important for ligand binding. We have now extended our mutagenesis analysis and identified additional residues which contribute to the Fas−FasL interaction. Candidate and control residues were selected based on a molecular model of the Fas extracellular region. Although residues in all three extracellular domains were identified to contribute to binding, the Fas−FasL interaction is centered on the second TNFR-like domain. Important residues were compared to critical positions in TNFR and CD40, another member of the TNFR family.

The interaction of Fas, a member of the tumor necrosis factor receptor (TNFR) family, with its TNF-like ligand (FasL),[1] provides a mechanism to control immune responses by apoptosis of Fas-expressing cells (*1*). The importance of the Fas−FasL system is demonstrated in the abnormal phenotypes generated in *lpr/lpr* (*2*) and *gld/gld* (*3*) mice, where mutation of the Fas or FasL genes prevents Fas-mediated apoptosis. Furthermore, the aberrant expression of FasL has been implicated in a number of disease processes, including a form of hepatitis (*4*, *5*), multiple sclerosis (*6*), Hashimoto's Thyroiditis (*7*), and neutrophil-mediated tissue damage of pulmonary tissue (*8*).

While structural details of the TNFR−TNF interaction have been elucidated by X-ray crystallography, knowledge of the Fas−FasL interaction at the molecular level is rudimentary. Therefore, by combining molecular modeling, site-specific mutagenesis, and a variety of binding assays, we have attempted to identify and characterize the ligand binding site in Fas. In an initial study, we have constructed a detailed three-dimensional (3D) model of the TNFR-homologous extracellular region of Fas (*9*). To support the modeling, we also studied residue (non) conservation in the TNFR family. Taken together, this knowledge was applied to aid in the identification of Fas residues important for ligand binding. By serine-scanning mutagenesis, we determined that two residues, R86 and R87, were critical for binding to FasL but not a panel of conformationally sensitive anti-Fas mAb (*10*). Four other Fas residues (K84, L90, E93, and H126) were found to support binding (*10*). These residues were predicted to form a binding surface involving parts of TNFR-homology domains 2 and 3 (D2 and D3) of Fas.

Here, we have extended our analysis of ligand binding to Fas. The aim of the current study was 2-fold. First, we wished to identify additional residues which contribute to the Fas−FasL interaction to obtain a more detailed picture of the Fas ligand binding site. Second, we intended to compare regions implicated in ligand binding to Fas with the ligand binding sites in TNFR and CD40. In this study, residues were selected for mutagenesis on the basis of our molecular model. Selection criteria were the predicted surface exposure of residues and their proximity to previously identified residues important for binding. Seven residues were subjected to mutagenesis. The generated mutant proteins were tested for binding to FasL and a panel of conformationally sensitive mAb. Three residues (R52, F81, and F117) were identified as important for the Fas−FasL interaction. Residues in all three TNFR-like extracellular domains (D1−D3) of Fas contribute to the interaction with FasL. However, the binding is centered on D2. A detailed spatial outline of the binding site was generated. Residues important for FasL binding are predicted to spatially correspond to critical sites in TNFR (*11*) and CD40 (*12*, *13*). These residues are largely conserved in human and mouse Fas but not conserved in TNFR or CD40.

MATERIALS AND METHODS

Molecular Model. For selection of residues for mutagenesis and mapping of the Fas ligand binding site, our previously reported 3D model of extracellular TNFR-

* Author to whom correspondence should be addressed. Bristol-Myers Squibb PRI, P.O. Box 4000, Princeton, NJ 08543. Phone: (609) 252-6269. Fax: (609) 252-6058. E-mail: starling@bms.com.

‡ University of Washington.

[1] Abbreviations: 3D, three-dimensional; CD40L, CD40 ligand; D1−3, extracellular tumor necrosis factor receptor-like domains 1−3; ELISA, enzyme-linked immunosorbant assay; HRP, horseradish peroxidase; FasL, Fas ligand; Ig, immunoglobulin; IgG, immunoglobulin G; mAb, monoclonal antibody; PBS, phosphate buffered saline; PCR, polymerase chain reaction; RT, room temperature; SDS−PAGE, sodium dodecyl sulfate−polyacrylamide gel electrophoresis; thr, thrombin cleavage site; TNF, tumor necrosis factor; TNFR, tumor necrosis factor receptor; wt, wild−type.

S0006-2960(97)02959-0 CCC: $15.00
Published on Web 02/24/1998

homology domains of Fas (*9*) was used. Briefly, the model was built by comparative modeling on the basis of multiple structure-oriented sequence comparison of TNFR family members and using X-ray structure coordinates of TNFR (*11*) as structural template. Computer graphics analysis of the model was carried out using InsightII (Version 95.0, MSI, San Diego, CA) on a Silicon Graphics (SGI) Indigo Impact. Color representations were produced using InsightII and processed as SGI RGB images.

Monoclonal Antibodies and Fusion Proteins. Soluble FasL was produced by fusing the extracellular domain of FasL to the extracellular domain of murine CD8 as previously described (*10, 14*). CD8-FasL was produced in COS cells following transfection by the DEAE-Dextran chloroquine method. Supernatants containing CD8-FasL fusion proteins were harvested and passed through a 0.22 μm filter. CD8-FasL was purified by affinity chromatography to immobilized 53-6 mAb (anti-murine CD8, gift from Diane Hollenbaugh, Bristol-Myers Squibb PRI).

A soluble protein (FasthrRγ1), consisting of the extracellular domain of Fas fused to the hinge, CH2 and CH3 regions of human IgG1 containing a thrombin cleavage site (thr), was constructed. Briefly, cDNA was amplified by PCR using oligonucleotide primers 5′-CGC CCC AAG CTT CGG AGG ATT GCT CAA CAA CC (containing a *Hin*dIII site) and 3′-CGC CGC GGA TCC CCC AAG TTA GAC CTG GAC CCT TCC TC (naturally occurring *Bam*HI and *Bgl*II sites were removed and a *Bam*HI site was added). Purified PCR products were digested with *Hin*dIII and *Bam*HI restriction enzymes, gel purified, and ligated into CDM7$^-$ containing a thr-human IgG1 (thrRγ1) cassette. Murine CD5thrRγ1, used as a negative control fusion protein, was prepared as previously described (*15*).

Site-Directed Mutagenesis. Seven amino acid residues in the extracellular domain of Fas were selected for site-directed mutagenesis to serine based on the molecular model of the Fas extracellular region (*9*). FasthrRγ1 mutants were produced by encoding the desired mutation in overlapping oligonucleotide primers, and using FasthrRγ1 cDNA as a template, the mutants were generated by PCR. The 5′ and 3′ oligonucleotide primers described for the production of FasthrRγ1 were also used for the generation of mutants. PCR products were digested with *Hin*dIII and *Bam*HI and ligated into the CDM7$^-$-thrRγ1 cassette as described above. Each cDNA construct was sequenced to confirm insertion of the appropriate mutation and to ensure that the PCR had not produced unwanted mutation. FasthrRγ1 and mutant supernatants were produced as described above for CD8-FasL, affinity purified on Protein A-sepharose, eluted with ImmunoPure elution buffer (Pierce, Rockford, IL), dialyzed in PBS and concentrated. Western blot analysis was performed to confirm that proteins were intact and no unexpected proteolysis had occurred in each purified protein sample.

Enzyme Immunoassays. Immulon 2 plates were coated overnight at 4 °C with 100 μL/well of 5 μg/mL donkey anti-human IgG (Jackson ImmunoResearch Labs., Inc., West Grove, PA) in 0.1 M sodium carbonate, pH 9.5. The plates were blocked for 2 h at 37 °C with 7.5% BSA in PBS and then washed 3 times with wash buffer (PBS containing 0.05% Tween 20, Sigma Chemical Co., St. Louis, MO). Various concentrations of protein A purified FasthrRγ1 fusion proteins were added to each well and incubated for 2 h at 37 °C prior to washing 6 times with wash buffer. A total of 100 μL of PBS containing 3% BSA and 2.5 μg/mL sFasL was added to each well, and the plates were incubated for 2 h at 37 °C. The plates were washed 6 times and then incubated with 1 μg/mL anti-FasL (Nok2, Pharmingen, San Diego, CA) for 2 h at 37 °C. The plates were washed 6 times, and bound anti-FasL mAb was detected with HRP-labeled sheep anti-mouse IgG. To directly quantitate the levels of the different FasthrRγ1 proteins bound to the plate, the Ig tail of the captured fusion protein was detected with sheep anti-human IgG (Amersham Corp., Arlington Heights, IL).

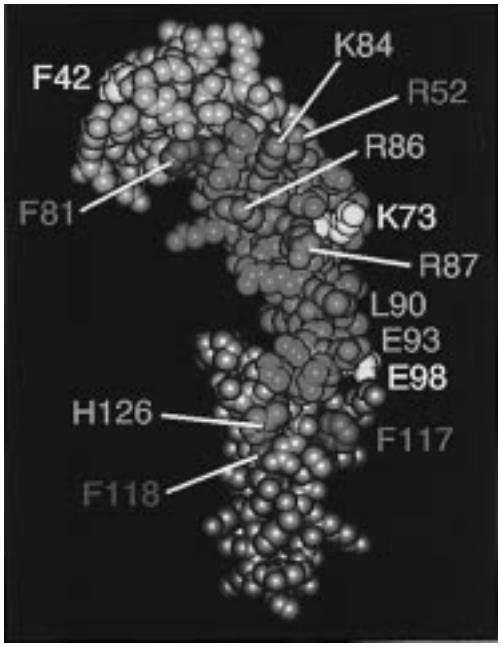

FIGURE 1: Mapping of mutated residues on a molecular model of the TNFR-homology domains of Fas. A space-filling representation is shown. TNFR-like domains 1−3 are colored gold (D1), blue (D2), and gray (D3). Residues previously identified as important for the Fas−FasL interaction are shown in magenta relative to (color-coded) residues which were targeted in this study (yellow, wt-like binding to ligand and mAb; red, wt level binding to mAb and significantly reduced binding to FasL; green, not expressed at detectable levels). The figure provides a spatial outline of the proposed ligand binding site in Fas (see text for details).

RESULTS AND DISCUSSION

Residue Selection. Seven residues were selected on the basis of our Fas molecular model (Figure 1) and mutated to serine. Five of these residues (R52, K73, F81, E98, and F117) mapped to solvent-exposed positions proximal to residues previously identified as important for the Fas−FasL interaction. Thus, these residues were likely candidates to participate in the receptor−ligand interaction. Residue F118 maps to a core position in the model. Mutation of this largely buried residue was therefore expected to severely compromise the 3D structure of Fas. In contrast, residue F42 maps to an exposed position somewhat distant from the putative ligand binding site, and its mutation was expected to neither compromise the structural integrity of Fas nor affect ligand binding. These residues were selected as controls and mutated to further test our model-based prediction of the FasL binding site.

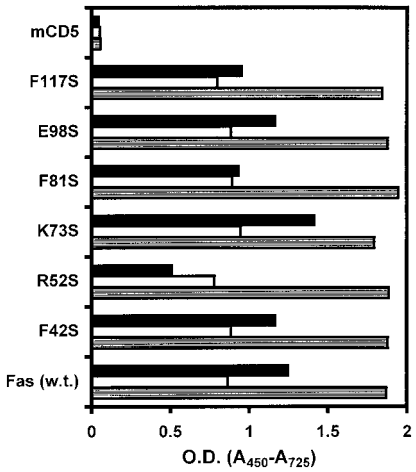

FIGURE 2: Binding of FasthrRγ1 and FasthrRγ1 mutant proteins to conformationally sensitive anti-Fas mAb by ELISA. Fusion proteins were immobilized on anti-human IgG coated plates, and binding was detected by the anti-Fas mAb noted at a concentration of 1ug/mL. Solid bars, SM1/1; open bars, SM1/17; striped bars, DX-2.

Mutagenesis and mAb Binding. The mutations were introduced by overlap extension PCR as described in the Materials and Methods section, and mutant proteins were expressed as soluble Ig fusion proteins. The mutant protein F118S was not expressed at levels able to be detected by either ELISA and Western Blot analysis, where we probed for presence of the IgG tail of the fusion protein. Therefore, mutation of this putative core residue severely compromised the integrity of the Fas protein, as expected. The structural integrity of all other mutant proteins was assessed by binding to a panel of conformationally sensitive mAb (Figure 2). Each of the six mutant proteins (with each mutated residue predicted to map to an exposed position) bound at wild-type levels to at least two of three mAb, indicating the absence of significant structural perturbations.

FasL Binding. The Fas mutant proteins were tested for ligand binding by ELISA (Figure 3). Two of the selected residues, F42 and R52, belong to TNFR-homology domain 1 (D1) of Fas, which was not considered in our initial study. As predicted, mutation of F42 to serine had little or no effect on ligand binding, whereas mutation of R52 significantly reduced binding of FasL (Figure 3). In the model, R52 in D1 is spatially adjacent to K84, which was found to contribute to FasL binding (*10*). K73 in D2 is proximal to R86 and R87, both of which are critical for the Fas−FasL interaction (*10*). However, mutation of K73 to serine had little effect on the ability to bind ligand or mAb (data not shown). Similarly, mutation of E98 to serine had essentially no effect on binding. In contrast, mutation of F81 in D2 and F117 in D3 resulted in significantly reduced binding, albeit at different levels (Figure 3). In the model, F117 is, in contrast to F118, solvent-exposed and its mutation only affected FasL binding but not the binding of the mAb. Thus, three residues (R52, F81, and F117) were identified as important for the Fas−FasL interaction. We had previously determined that the K_d value for the interaction of wild-type FasthrRγ1 with FasL was about 7×10^{-8} by Biacore analysis (*10*). On the basis of comparisons of values for 50% binding in the ELISA studies (comparison with the parent FasthrRγ1), the mutations at positions F42 and K73 did not noticeably

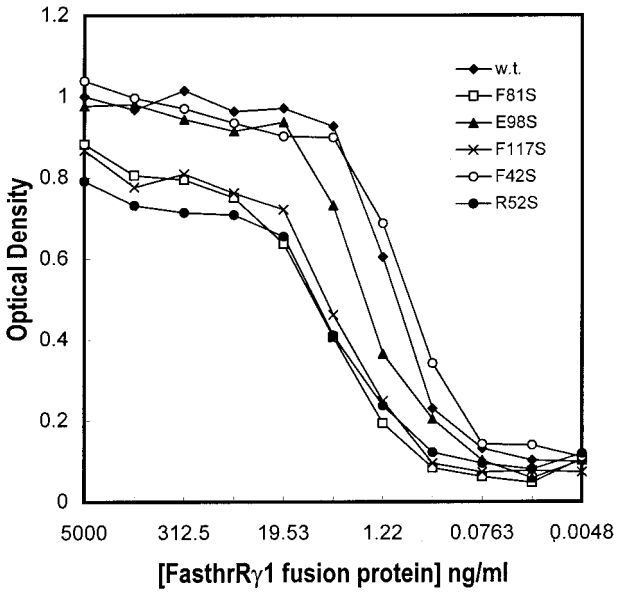

FIGURE 3: Binding of FasL to immobilized FasthrRγ1 mutants in ELISA. Protein A-purified fusion proteins were captured on ELISA plates at the concentrations noted using donkey anti-human IgG. Purified soluble CD8- FasL (2.5 μg/mL) was added to plates, and binding of FasL was detected using the Nok-2 mAb (1 μg/mL) and HRP-conjugated anti-mouse IgG (1/5000). Mutant K73S exhibited wild-type (wt) binding of sFasL (data not shown).

effect binding; the mutation at position E98 reduced binding affinity to a small extent (less than 3-fold weaker binding in the experiment represented in Figure 3). However, mutation to serine at positions F117, F81, and R52 decreased binding in a reproducible manner (7.5, 12, and 14-fold, respectively, in the experiment represented in Figure 3). Bioassay of the ability of the proteins to inhibit FasL-mediated death of Jurkat cells showed a similar hierachy of responses (data not shown).

The FasL Binding Site. In Figure 1, we have mapped residues important for the Fas−FasL interaction, as identified by mutagenesis, ligand, and mAb binding assays, on our Fas molecular model. The ability to accurately predict the effects of mutations of residues (F42, R52, F81, F117, and F118) assigns confidence to our prediction of the FasL binding site. Six previously identified residues important for the Fas−FasL interaction are, with no exception, conserved in mouse and human Fas, consistent with the presence of cross-species Fas−FasL interactions. F117 is also conserved, while R52 and F81 are conservatively replaced (R/K and F/Y, respectively) in human and mouse Fas. Taken together, our studies have, despite their limitations, enabled us to obtain a relatively detailed picture of the putative FasL binding site (Figure 1). In the model, residues important for FasL binding map to one face of the molecule and form a coherent binding surface. We have identified residues in all three TNFR-homology domains which contribute to the interaction. The majority of these residues map to domain D2, which is thought to provide the center of the Fas−FasL interaction.

Residues Important for Ligand Binding to TNFR Family Members. Structural studies on the TNFR-TNF interaction (*11*) and mutagenesis studies on the CD40−CD40L (*12*, *13*) and Fas−FasL interactions (*10* and references presented herein) have identified residues important for ligand binding to these receptors. A common feature of these receptor interactions is that the majority of important residues map

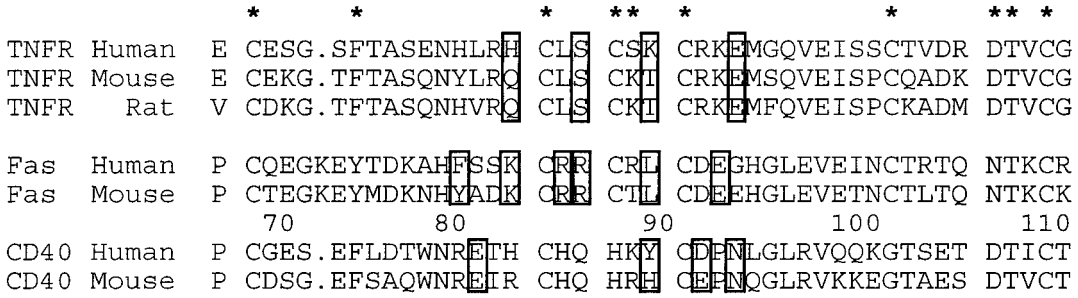

FIGURE 4: Structure-oriented comparison of domain D2 sequences of TNFR, Fas, and CD40 molecules from different species. Positions thought to be critical for maintaining the integrity of the TNFR fold are labeled with asterisks. Fas and CD40 sequences were aligned with TNFR using these residues as anchor points. Thus, the alignment of residues implies approximate topological equivalence. TNFR residues most buried (>60 Å^2 solvent-accessible surface) in the TNFR−TNF complex X-ray structure (*11*) are boxed. D2 residues in human Fas and human CD40 which are, on the basis of mutagenesis, most important for the Fas−FasL and CD40−CD40L interaction, respectively, are also boxed.

to the second TNFR-like domains of the receptors. We have compared the most important sites with a structure-oriented sequence alignment of D2 in TNFR, CD40, and Fas molecules from different species (Figure 4). Highlighted are residues most involved in the interactions, as determined by structural or mutagenesis analysis. This comparison suggests that residues which determine ligand binding to Fas map to positions in the central region of D2 and approximately spatially correspond to critical residues in TNFR and CD40. Thus, the binding sites in these TNFR family members are very likely to involve corresponding regions. Most of the compared residues are conserved or conservatively replaced in homologues from different species but differ between the receptors. This provides an explanation for the specificity of the respective receptor−ligand interactions. The conservation of important residues in human and mouse Fas is also consistent with the presence of cross-species Fas−FasL interactions (*16*). In addition, the comparison suggests that residues in this region of other TNFR-like receptors are likely to determine ligand binding. Thus, these findings are expected to aid in the identification of ligand binding sites in other TNFR superfamily members.

ACKNOWLEDGMENT

We would like to thank Steve Farris for help in preparing and sequencing cDNA constructs, Steve Kosowski for preparation of fusion proteins, and Vina Patil-Koota for assistance with ELISA.

REFERENCES

1. Nagata, S., and Golstein, P. (1995) *Science 267*, 1449−1456.
2. Watanabe-Fukunaga, R., Brannan, C. I., Copeland, N. G., Jenkins, N. A., and Nagata, S. (1992) *Nature 356*, 314−317.
3. Takahashi, T., Tanaka, M., Brannan, C. I., Jenkins, N. A., Copeland, N. G., Suda, T., and Nagata, S. (1994) *Cell 76*, 969−976.
4. Ogasawara, J., Watanabe-Fukunaga, R., Adachi, M., Matsuzawa, A., Kasugai, T., Kitamura, Y., Itoh, N., Suda, T., and Nagata, S. (1993) *Nature 364*, 806−809.
5. Galle, P. R., Hofmann, W. J., Walczak, H., Schaller, H., Otto, G., Stremmel, W., Krammer, P. H., and Runkel, L. (1995) *J. Exp. Med. 182*, 1223−1230.
6. Dowling, P., Shang, G., Raval, S., Menonna, J., Cook, S., and Husar, W. (1996) *J. Exp. Med. 184*, 1513−1518.
7. Giordano, C., Stassi, G., De Maria, R., Todaro, M., Richiusa, P., Papoff, G., Ruberti, G., Bagnasco, M., Testi, R., and Galluzzo, A. (1997) *Science 275*, 960−963.
8. Liles, W. C., Kiener, P. A., Ledbetter, J. A., Aruffo, A., and Klebanoff, S. J. (1996) *J. Exp. Med.* 184, 429−440.
9. Bajorath, J., and Aruffo, A. (1997) *J. Computer-Aided Mol. Des. 11*, 3−8.
10. Starling, G. C., Bajorath, J., Emswiler, J., Ledbetter, J. A., Aruffo, A, and Kiener P. A. (1997) *J. Exp. Med. 185*, 1487−1492.
11. Banner, D. W., D'Arcy, A., Janes, W., Gentz, R., Schoenfeld, H.-J., Broger, C., Loetscher, H., and Lesslauer. W. (1993) *Cell* 73, 431−445.
12. Bajorath, J., Chalupny, N. J., Marken, J. S., Siadak, A. W., Skonier, J., Gordon, M., Hollenbaugh, D., Noelle, R. J., Ochs, H. D., and Aruffo A. (1995) *Biochemistry 34*, 1833−1840.
13. Bajorath, J., Marken, J. S., Chalupny, N. J., Spoon, T. L., Siadak, A. W., Gordon, M., Noelle, R. J., Hollenbaugh, D., and Aruffo, A. (1995) *Biochemistry 34*, 9884−9892.
14. Kiener, P. A., Davis, P. M., Starling, G. C., Mehlin, C., Klebanoff, S. J., Ledbetter, J. A., and Liles, W. C. (1997) *J. Exp. Med. 185*, 1511−1516.
15. Starling, G. C., Llewellyn, M. C., Whitney, G. S., and Aruffo, A. (1997) *Tissue Antigens 49*, 1−6.
16. Takahashi, T., Tanaka, M., Inazawa, J., Abe, T., Suda, T., and Nagata, S. (1994) *Int. Immunol. 6*, 1567−1574.

BI972959D